

**EFFECTS OF CUTTING STRATEGY IN THE CONTOUR
MILLING OF OPEN POCKET AISI H13 WITH A LOW
RATIO THIN-WALLED FEATURE**

BY

AVICENNA

**A thesis submitted in fulfilment of the requirement for the
degree of Doctor of Philosophy (Engineering)**

**Kulliyyah of Engineering
International Islamic University Malaysia**

MARCH 2022

ABSTRACT

In the pocket machining of hard material with a thin-walled structure, the selection of cutting strategy and conditions significantly influences the process, machined part, and tool condition outputs. Variations in cutting engagement variables, including cutting speed, feed rate, and depth of cut, could either significantly improve or deteriorate the cutting time components, machined part quality, and tool conditions to certain levels. This research combined the roughing and finishing operations in the pocket milling of hardened AISI H13 tool steel. Two consecutive cutting processes, with different contour tool paths, were integrated into a single operation (run) made for two distinct features of open pocket lateral wall and low-ratio thin-walled feature.

The organisation of the research was made into two consecutive parts. The first part was carried out entirely through the conduct of virtual machining for the development of tool path and the investigation of simulated machining time, while the second part was focused on the actual machining to collect experimental data for the characterisation of the process, workpiece and tool wear. Supersaturated response surface methods: Definitive screening design (DSD) was used as the experimental design where eleven independent variables were employed for the virtual machining, and six independent variables were employed for the actual cutting processes.

The simulated feeding time and rapid time results indicated that the axial and radial depth of cuts, the incremental distance of feeding and rapid planes, as well as the fixed components and rapid traverse speed overrides were among the variables that contributed to the tool path length; hence, increasing the machining time. In terms of actual machining, the significant variables for the open pocket wall machining were (1) cutting speed $v_c(OP)$, (2) feed rate $v_f(OP)$, (3) and depth-of-cut for finishing operation DOC_f , and for the thin-walled feature machining were (1) the depth-of-cut for roughing operation DOC_r , (2) cutting speed $v_c(TW)$, (3) and feed rate $v_f(TW)$. The observations on cutting temperature suggested that the two cutting processes of open pocket wall and thin-walled feature differed due to the different radial depth of cut. The maximum observable cutting temperature for the machining of the open pocket wall was 278.1 °C, while the thin-walled feature was 107.9 °C. The surface roughness was ranged from 0.09 to 0.27 μm for the pocket floor, 0.35 to 2.03 μm for the lateral pocket wall, and 0.15 to 1.58 μm for the thin-walled feature. Furthermore, the observations on mechanical surface alterations showed the presence of built-up edge, burr, and feed marks in almost all experimental runs.

The findings of this research were expected to be useful for other researchers and industrial practitioners by providing valuable multiple data that could act as a point of reference in carrying out similar processes. In this case, the research parameters can be further adapted for the production of parts with certain desired outputs, particularly in terms of machined part tolerances, allowances, and surface roughness. Furthermore, the data from tool damage observations can also be adopted to further develop the tool life estimation from the application of a similar tool class.

خلاصة البحث

عند تشكيل التجويف للمواد الصلبة بهيكل رقيق الجدار، يؤثر اختيار استراتيجية القطع وظروفها بشكل كبير على العملية والجزء المشكّل ومخرجات حالة الأداة. يمكن أن تؤدي الاختلافات في متغيرات المشاغلة، بما في ذلك سرعة القطع ومعدّل التغذية وعمق القطع، إلى تحسين أو تدهور عناصر زمن القطع وجودة الأجزاء المشكّلة وحالة الأداة إلى حدّ معين. دمج هذا البحث بين عمليات التخشين والصّقل في التجويف الآلي لأداة الفولاذ AISI H13 الصلبة. تم دمج عمليتي قطع متتاليتين، مع مسارات محيطية مختلفة للأداة، في عملية واحدة (شغل) صنّعت لميزتين بارزتين للجدار الجانبي للتجويف المفتوح وخاصة الجدران الرقيقة منخفضة النسبة.

تم تنظيم البحث في جزأين متتاليتين. تمّ تنفيذ الجزء الأول بالكامل من خلال إجراء معالجة افتراضية لتطوير مسار الأداة والتحقق في زمن المعالجة المحاكاة، بينما ركّز الجزء الثاني على المعالجة الفعلية لجمع البيانات التجريبية لتوصيف العملية وقطعة التشغيل وتلف أداة القطع. طرق سطح الاستجابة المفرطة التشعب: تم استخدام تصميم الفحص المحدّد (DSD) كتنصميم تجريبي حيث تم توظيف أحد عشر متغيراً مستقلاً للمعالجة الافتراضية وستّ متغيرات مستقلة لعمليات القطع الفعلية.

أشارت نتائج وقت التغذية المحاكي والوقت السريع إلى أن العمق المحوري والشعاعي للقطع، والمسافة المتزايدة للتغذية والمستويات السريعة، بالإضافة إلى العناصر الثابتة وقيمة تجاوز سرعة التمرير كانت من بين المتغيرات التي ساهمت في طول مسار الأداة؛ وبالتالي، زيادة زمن المعالجة. فيما يتعلق بالآلات الفعلية، كانت المتغيرات المهمة لتشكيل جدار التجويف المفتوح هي (1) سرعة القطع $v_c(OP)$ ، (2) معدّل التغذية $v_f(OP)$ ، (3) وعمق القطع DOC_r لإنهاء عملية الصّقل، بينما لميزة الجدران الرقيقة كانت المتغيرات (1) عمق القطع لعملية التخشين DOC_r ، (2) سرعة القطع $v_c(TW)$ ، (3) ومعدّل التغذية $v_f(TW)$. اقترحت الملاحظات على درجة حرارة القطع أن عمليتي القطع لجدار التجويف المفتوح وخاصة الجدران الرقيقة اختلفتا بسبب اختلاف العمق الشعاعي للقطع. كانت أقصى درجة حرارة قطع يمكن ملاحظتها لتشكيل جدار التجويف المفتوح 278.1 درجة مئوية، بينما كانت لميزة الجدران الرقيقة 107.9 درجة مئوية. تراوحت خشونة السطح من 0.09 إلى 0.27 ميكرومتر لأرضية التجويف، ومن 0.35 إلى 2.03 ميكرومتر لجدار التجويف الجانبي، ومن 0.15 إلى 1.58 ميكرومتر لميزة الجدران الرقيقة. علاوة على ذلك، أظهرت الملاحظات على التعديلات الميكانيكية السطحية وجود حافة مدججة وعلامات تنوء وتغذية في جميع الأشواط التجريبية تقريباً.

كان من المتوقع أن تكون نتائج هذا البحث مفيدة للباحثين والممارسين الصناعيين من خلال توفير بيانات متعددة قيمة يمكن أن تكون بمثابة نقطة مرجعية في تنفيذ عمليات مماثلة. وفي هذه الحالة، يمكن ملاءمة متغيرات البحث لإنتاج أجزاء ذات نواتج مرغوبة، لاسيما فيما يتعلق بتفاوتات الأجزاء المشكّلة والبدلات وخشونة السطح. علاوة على ذلك، يمكن أيضاً اعتماد البيانات من ملاحظات تلف أداة القطع لمواصلة تطوير تقدير عمر الأداة من تطبيق فئة أداة مماثلة.

APPROVAL PAGE

The thesis of Avicenna has been approved by the following:

Erry Yulian T. Adesta
Supervisor

Mohd. Radzi Hj. Che Daud
Co-Supervisor

Md. Yusof Ismail
Internal Examiner

Awaluddin Mohamed Shaharoun
External Examiner

Ing. Yupiter H. P. Manurung
External Examiner

Sohirin Mohd Solihin
Chairman

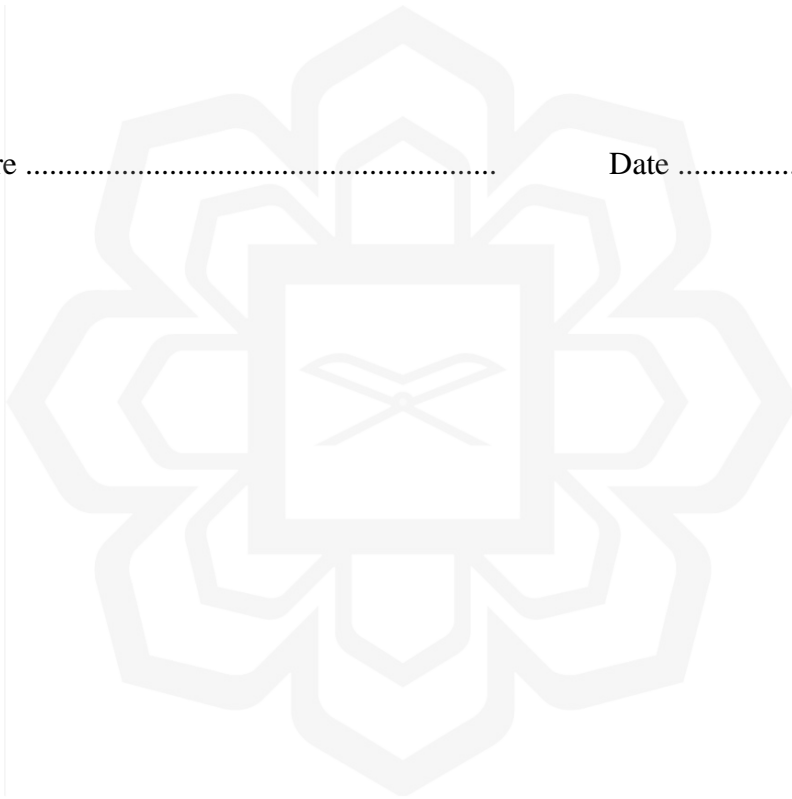
DECLARATION

I hereby declare that this thesis is the result of my own investigations, except where otherwise stated. I also declare that it has not been previously or concurrently submitted as a whole for any other degrees at IIUM or other institutions.

Avicenna

Signature

Date



INTERNATIONAL ISLAMIC UNIVERSITY MALAYSIA

**DECLARATION OF COPYRIGHT AND AFFIRMATION OF
FAIR USE OF UNPUBLISHED RESEARCH**

**EFFECTS OF CUTTING STRATEGY IN THE CONTOUR
MILLING OF OPEN POCKET AISI H13 WITH A LOW RATIO
THIN-WALLED FEATURE**

I declare that the copyright holders of this thesis are jointly owned by the student and IIUM.

Copyright © 2022 Avicenna and International Islamic University Malaysia.
All rights reserved.

No part of this unpublished research may be reproduced, stored in a retrieval system, or transmitted, in any form or by any means, electronic, mechanical, photocopying, recording or otherwise without prior written permission of the copyright holder except as provided below

1. Any material contained in or derived from this unpublished research may be used by others in their writing with due acknowledgement.
2. IIUM or its library will have the right to make and transmit copies (print or electronic) for institutional and academic purposes.
3. The IIUM library will have the right to make, store in a retrieved system and supply copies of this unpublished research if requested by other universities and research libraries.

By signing this form, I acknowledged that I have read and understood the IIUM Intellectual Property Right and Commercialization policy.

Affirmed by (Avicenna)

.....
Signature

.....
Date

ACKNOWLEDGEMENT

Alhamdulillah, I praise and thank Allah (glory be to Him) for His greatness, and for the strength given to me in this endless quest of knowledge pursuit. It is only by His countless blessings and mercy that I managed to complete and publish this thesis.

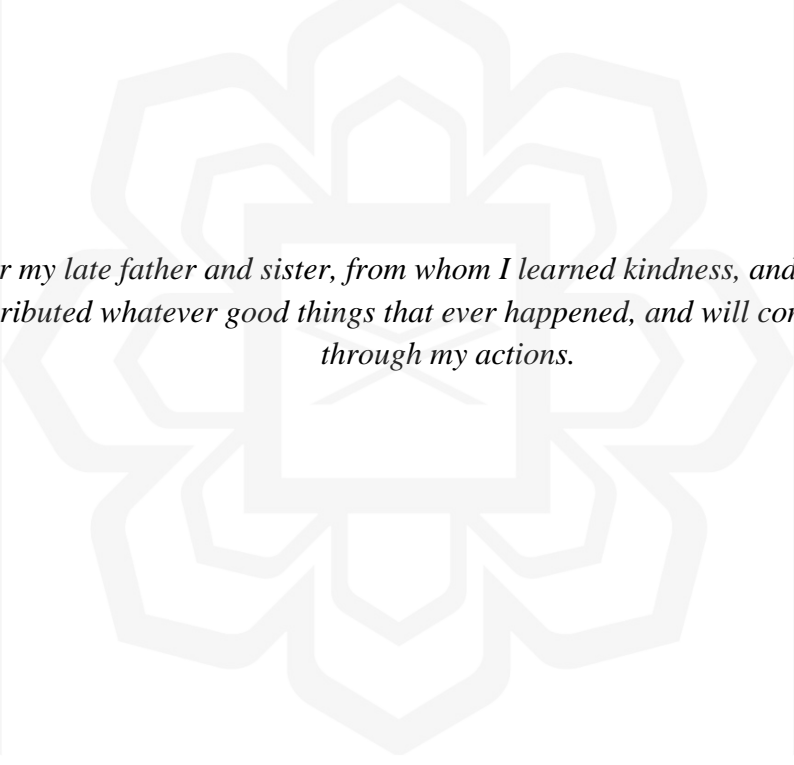
First and foremost, my sincerest gratitude to my supervisor, Prof. Dr. Erry Y. T. Adesta, who has given me the invaluable opportunity to continue my education under his guidance and supervision. I am privileged and indebted for all the experience and lessons learned from his sophistication and savoir-faire. My sincere appreciation also goes to Assoc. Prof. Dr. Mohd Radzi B Che Daud, who has been sharing his extensive knowledge and experience. They are all thought-provoking and informative for the expansion of my horizon.

I also owe my gratitude to all staff in the Kulliyah of Engineering, the Department of Manufacturing and Materials Engineering, and the Department of Science in Engineering, who have been assisting and supporting me through their kind understanding: Dr. Raihan Othman, Dr. Mohd Lukman Inche Ibrahim, Dr. Sany Izan Ihsan, Dr. Siti Fauziah Toha, Dr. Mohamed Abd. Rahman, and all the staff members of the three offices I could not mention one by one. Special appreciation also goes to Brother Syed Mohammad Khairuddin for his technical assistance and guidance in the laboratory, as well as Sister Siti Salwiah Shukri and Sister Sharifah Hussain for the push, reminders, and administrative assistance. Without them, this thesis would be hardly compiled.

My special warm thanks to all of my family members to whom I am deeply in debt. The journey has been taking way too long, and I am so grateful for all their patience and support. The last few years have been rough, and I am still far from being helpful. The honourable mention goes to my late father and sister, for their spirits and fond memories, so I can keep moving forward.

Lastly, to everyone that I could not mention one by one, thank you is not really enough to express how grateful I am. I shall remember all their assistance and support and cherish them as I embark on the new chapter of life.

“...And when ye are told to rise up, rise up. Allah will raise up, to (suitable) ranks (and degrees), those of you who believe and who have been granted (mystic) Knowledge. And Allah is well-acquainted with all ye do” [Quran, 58: 11]



For my late father and sister, from whom I learned kindness, and to whom I attributed whatever good things that ever happened, and will come to pass, through my actions.

TABLE OF CONTENTS

Abstract	ii
Abstract in Arabic	iii
Approval Page.....	iv
Declaration	v
Copyright	vi
Acknowledgement	vii
Table of Contents	ix
List of Tables	xiii
List of Figures	xvi
List of Abbreviations	xxiii
List of Symbols	xxiv
CHAPTER ONE: INTRODUCTION	1
1.1 Background of the Study	1
1.2 Problem Statement.....	3
1.3 Research Philosophy.....	4
1.4 Research Objectives.....	7
1.5 Research Scope.....	7
1.6 Research Hypothesis.....	10
1.7 Significance of the Study.....	10
1.8 Thesis Organisation	12
CHAPTER TWO: LITERATURE REVIEW	14
2.1 Introduction to Machining	14
2.1.1 Fundamental of Machining Processes.....	14
2.1.2 Milling.....	18
2.1.2.1 Classification of Milling Types and Operations.....	18
2.1.2.2 Cutting Kinematics	21
2.1.2.3 Cutting Parameters	24
2.1.2.3.1 Cutting Force	25
2.1.2.3.2 Cutting Speed and Spindle Speed	26
2.1.2.3.3 Feed Rate	27
2.1.2.3.4 Depth of Cut.....	29
2.1.2.3.5 Tool Path.....	31
2.2 Machining of Hard Materials	35
2.2.1 Machine Tools, Cutting Tools, and Materials.....	37
2.2.2 Characteristics of Hard Machining Processes.....	39
2.2.2.1 Cutting Forces	40
2.2.2.2 Chip Formation.....	40
2.2.2.3 Cutting Temperature.....	41
2.2.2.4 Ceramic and PCBN Tool Wear	43
2.2.2.5 Modelling of Cutting Process	45
2.2.3 Hard Machining for Mould and Dies.....	47
2.2.4 Recent Advances in Contour and Thin-Walled Milling Operations.....	48

2.3	Tool Geometry, Material, and Wear.....	52
2.3.1	Tool Geometry	52
2.3.2	Tool Materials	57
2.3.2.1	High-Speed Steels (HSS)	58
2.3.2.2	Cast Non-Ferrous Alloys.....	59
2.3.2.3	Sintered Carbides.....	60
2.3.2.4	Ceramics	62
2.3.2.5	Cubic Boron Nitride	63
2.3.2.6	Diamond	64
2.3.3	Tool Wear.....	65
2.3.3.1	Tool Damages Regulated by Cutting Temperature.....	68
2.3.3.2	Tool Wear Mechanisms, Locations, and Measurements.....	73
2.3.3.3	Tool Wear Evolution	77
2.4	Workpiece Material	79
2.4.1	Metal Workpiece.....	80
2.4.2	Tool Steels.....	81
2.4.3	Machinability of Work Material	83
2.4.4	Surface Overview.....	84
2.4.4.1	Surface Texture	86
2.4.4.2	Surface Roughness and Surface Finish	88
2.4.4.3	Surface Integrity	91
2.4.5	Machining Defects	92
2.4.5.1	Burr Formation	92
2.4.5.2	Surface Cracks.....	94
2.4.5.3	Built-up Edge (BUE).....	94
2.5	Virtual Machining.....	95
2.5.1	Computer-Aided Design and Manufacturing System.....	99
2.6	Design of Experiment.....	100
2.6.1	Response Surface Methodology.....	102
2.6.2	Supersaturated RSM: Definitive Screening Designs	104
2.6.3	Statistical Analysis	107
2.7	Chapter Summary	110
CHAPTER THREE: RESEARCH METHODOLOGY		112
3.1	Organisation of the Research.....	113
3.2	Research Materials.....	115
3.2.1	Workpiece Material and Properties.....	115
3.2.2	Milling Insert.....	117
3.3	Equipment and Tools.....	118
3.3.1	Machining Process	118
3.3.1.1	Machining Centre	118
3.3.1.2	Cutting Tool.....	119
3.3.2	Observation and Measurement for Machining Results.....	120
3.3.2.1	IR Thermographic Camera	121
3.3.2.2	Surface Roughness Tester	122
3.3.2.3	Calliper	123
3.3.2.4	Microscope	124
3.3.3	Virtual Machining and Data Analysis.....	124
3.3.3.1	Computer-Aided Design (CAD) Software	125

3.3.3.2 Computer-Aided Manufacturing (CAM) Software	125
3.3.3.3 Statistical Software Package.....	125
3.3.3.4 Spreadsheet and Word Processor	125
3.4 Experimental Setup.....	126
3.5 Cutting Profile and Tool Path.....	128
3.6 Design of Experiment (DOE)	131
3.6.1 DOE for Research Part I	132
3.6.2 DOE for Research Part II.....	136
3.7 Data Analysis.....	139
3.8 Chapter Summary	140
CHAPTER FOUR: RESULTS AND DISCUSSION	141
4.1 PART 1 – Virtual Machining Analysis	141
4.1.1 Selection of Cutting Tool Path.....	141
4.1.2 Feeding Time Analysis	149
4.1.2.1 Analysis of Variance and Fit Statistics.....	151
4.1.2.2 Model Diagnostics.....	153
4.1.2.3 Significant Parameters in Feeding Time	163
4.1.3 Rapid Time Analysis.....	170
4.1.3.1 Analysis of Variance, Fit Statistics, and Model Diagnostics.....	171
4.1.3.2 Significant Factors in Rapid Time.....	173
4.1.4 Machining Time	181
4.2 PART 2 – Actual Machining Analysis	184
4.2.1 Cutting Temperature	185
4.2.1.1 Cutting Temperature During Machining of Pocket Wall	186
4.2.1.2 Cutting Temperature During Machining of Thin-Walled Feature	194
4.2.1.3 Cutting Temperature Transitions.....	201
4.2.2 Machined Surface Quality.....	205
4.2.2.1 Thin-Walled Feature-related Dimensions	205
4.2.2.1.1 Dimension Deviations of Thin-Walled Feature	206
4.2.2.1.2 Relative Position of Thin-walled Feature	213
4.2.2.1.3 Analysis of Machining Dimension Deviations	218
4.2.2.2 Surface Roughness	221
4.2.2.2.1 Surface Roughness of Pocket Floor	222
4.2.2.2.2 Surface Roughness of Lateral Pocket Wall	225
4.2.2.2.3 Surface Roughness of Thin-Walled Feature	231
4.2.2.3 Mechanical Surface Alterations	238
4.2.2.3.1 Lay Conditions.....	238
4.2.2.3.2 Built-Up Edge Formation	240
4.2.2.3.3 Burr Formation.....	243
4.2.2.3.4 Feed Marks and Stress Patterns	245
4.2.3 Tool Damage.....	247
4.2.3.1 Flank Wear	247
4.2.3.2 Rake Damage.....	251
4.3 Chapter Summary	254

CHAPTER FIVE: CONCLUSIONS AND RECOMMENDATIONS	256
5.1 Conclusions	256
5.2 Limitation of the Study	259
5.3 Recommendations.....	260
REFERENCES.....	262
APPENDICES	273
Appendix 1: Diagnostics summary for Rapid Time <i>RT</i> (Research Part I) with square root transformation.....	273
Appendix 2: Normal Probability, Residuals vs. Predicted, and Box-Cox Plots for Rapid Time <i>RT</i> model in Research Part I	274
Appendix 3: Maximum temperature T_c in the machining processes of the pocket wall (OP) and thin-walled (TW) features.	276
Appendix 4: Normal distribution and residuals vs. predicted plots of cutting temperature T_c (OP) in the machining of pocket wall feature	277
Appendix 5: Normal distribution and residuals vs. predicted plots of cutting temperature T_c (OP) in the machining of pocket wall feature	278
Appendix 6: Normal plot of residuals for reduced quadratic model of width deviation W_w	279
Appendix 7: Normal plot of residuals for reduced quadratic model of width deviation W_{pw}	280
Appendix 8: Normal plot of residuals for reduced linear model of surface roughness $Ra(FL)$	281
Appendix 9: Normal plot of residuals for reduced quadratic model of surface roughness $Ra(OP)$	282
Appendix 10: Normal plot of residuals of reduced quadratic model for surface roughness $Ra(TW)$	283

LIST OF TABLES

Table 2.1	AISI tool steels prefix, their typical compositions, and hardness (Adapted from Groover (2020))	83
Table 3.1	Descriptive summary of the research organisation, arranged in two-parts executable processes	112
Table 3.2	Chemical composition of AISI H13 steel (Perez et al., 2015; Telasang et al., 2014; Taktak et al., 2007)	115
Table 3.3	Machine specifications of Mazak Nexus 410A-II (Mazak Corporation, 2014)	119
Table 3.4	Technical specifications of ThermoPro™ TP8 (Thermo-Delta Kft., n.d.)	122
Table 3.5	Technical specifications of Mitutoyo Surftest SV-3200 (Mitutoyo U.S.A, n.d.-b)	123
Table 3.6	Technical specifications of <i>Mitutoyo ABS Digimatic Caliper</i> (Mitutoyo U.S.A, n.d.-a)	123
Table 3.7	Technical specifications of Nikon Measuring Microscopes MM-400/L Trinocular Head (Nikon, 2019)	124
Table 3.8	Summary of experimental design layout for Research Part I.	135
Table 3.9	Summary of experimental design layout for Research Part II.	137
Table 4.1	Experimental design of the machining parameters and the simulated response of feeding time <i>FT</i>	150
Table 4.2	ANOVA for the linear model of feeding time <i>FT</i>	151
Table 4.3	Fit Statistics for the ANOVA results of feeding time response.	152
Table 4.4	Diagnostics summary for feeding time <i>FT</i> (Research Part I) with no response transformations	153
Table 4.5	Modified ANOVA for the linear model of feeding time <i>FT</i> (Research Part I) (Transformation: Natural Log)	158
Table 4.6	Fit Statistics for modified ANOVA results of feeding time response (Transformation: Natural Log)	159

Table 4.7	Diagnostics summary for feeding time FT (Research Part I) with Natural Log response transformations	160
Table 4.8	Experimental design of the machining parameters and the simulated response of rapid time RT	170
Table 4.9	ANOVA for the linear model of rapid time RT (Research Part I)	171
Table 4.10	Fit Statistics for the ANOVA results of rapid time RT	172
Table 4.11	Mean values of observed maximum cutting temperature during pocket wall (OP) and thin wall (TW) machining processes	186
Table 4.12	ANOVA for reduced quadratic model of cutting temperature $T_c(OP)$ during pocket wall machining	187
Table 4.13	Fit Statistics for ANOVA results of cutting temperature $T_c(OP)$ response	188
Table 4.14	ANOVA for reduced quadratic model of cutting temperature $T_c(TW)$ during thin wall machining	194
Table 4.15	Fit Statistics for ANOVA results of cutting temperature $T_c(TW)$ response	195
Table 4.16	Mean deviations of thin-walled feature width W_w and pocket-to-thin-walled feature distance W_{pw}	206
Table 4.17	ANOVA for reduced quadratic model of deviation W_w during thin wall machining	207
Table 4.18	Fit Statistics for ANOVA results of reduced quadratic model of dimension deviation W_w .	207
Table 4.19	ANOVA for reduced quadratic model of deviation W_{pw} during thin wall machining	214
Table 4.20	Fit Statistics for ANOVA results of reduced quadratic model of dimension deviation W_{pw}	214
Table 4.21	Mean surface roughness of pocket floor $Ra(FL)$, pocket wall $Ra(OP)$, and thin wall $Ra(TW)$ features	222
Table 4.22	ANOVA for reduced linear model of mean surface roughness $Ra(FL)$	222
Table 4.23	Fit Statistics for ANOVA results of surface roughness $Ra(FL)$ response	223

Table 4.24	ANOVA for reduced quadratic model of mean surface roughness $Ra(OP)$	226
Table 4.25	Fit Statistics for ANOVA results of surface roughness $Ra(OP)$ response	226
Table 4.26	ANOVA for reduced quadratic model of mean surface roughness $Ra(TW)$	232
Table 4.27	Fit Statistics for ANOVA results of surface roughness $Ra(TW)$ response	233



LIST OF FIGURES

Figure 2.1	The orthogonal (a and b), non-orthogonal (c), and semi-orthogonal (d) metal cutting process (Childs et al., 2000).	15
Figure 2.2	Effective zones in chip formation and derived model of deformation in the shear plane (Böllinghaus et al., 2009)	17
Figure 2.3	Comparison of face milling and peripheral milling (Böllinghaus et al., 2009).	19
Figure 2.4	Comparison of down- and up-milling (DIN 6580E) (Böllinghaus et al., 2009)	20
Figure 2.5	Four milling operations of: (a) Face milling, (b) Shoulder milling, (c) Peripheral milling, and (d) Ball-end milling (Lopez de Lacalle, Campa, et al., 2011).	21
Figure 2.6	Tool-workpiece engagement variables in plain face milling (Böllinghaus et al., 2009)	23
Figure 2.7	The difference between peripheral milling and slotting, and how axial depth of cut (ADOC) and radial depth of cut (RDOC) relate to the operation (Harvey Performance, 2017)	30
Figure 2.8	Typical boundary offsetting problems for closed curves (Dhanik & Xirouchakis, 2010).	33
Figure 2.9	(a) Common wear pattern to be found on a PCBN tool when producing saw-tooth chip (Tönshoff et al., 2000) and (b) the visualization of notch wear on the secondary flank face of a tooth	44
Figure 2.10	Finite element modelling of (a) chip formation, (b) distribution of temperature, and (c) surface finish (Ng & Aspinwall, 2002; Özel et al., 2007).	46
Figure 2.11	Double-sided milling concept in dual parallel kinematic machines approach	51
Figure 2.12	Reference planes in cutting tool geometry (Astakhov & Davim, 2008)	54
Figure 2.13	Multi-axis milling tool of (a) flat end cutter, (b) fillet end cutter, and (c) ball end cutter (Qiao et al., 2019).	56

Figure 2.14	Tool wear and failure types (adapted from Sandvik®) (Astakhov & Davim, 2008)	66
Figure 2.15	Cutting tool wear and loading types (Böllinghaus et al., 2009)	68
Figure 2.16	Correlation between cutting temperature and damage removal rate in adhesion, mechanical damage, and thermal damage mechanisms (T. Childs et al., 2000c).	69
Figure 2.17	Four types of tool damage in terms of sizes (T. Childs et al., 2000c).	71
Figure 2.18	ISO 8688 end milling tool wear (Lopez de Lacalle, Lamikiz, et al., 2011).	75
Figure 2.19	(a) Uniform chipping <i>CH1</i> and (b) non-uniform chipping <i>CH2</i> according to ISO 8688 (Lopez de Lacalle, Lamikiz, et al., 2011).	76
Figure 2.20	ISO 3685:1993 four tool wear zones and types (Astakhov & Davim, 2008).	77
Figure 2.21	Tool wear curves in the forms of (a) normal wear and (b) evolution of flank wear <i>VB_B</i> in different cutting speeds as a cutting time function (Astakhov & Davim, 2008).	79
Figure 2.22	Cross-section diagram of a typical metallic part surface (Groover, 2020).	85
Figure 2.23	The major constituents that comprise a typical surface: Profile, Waviness and Roughness, indicating a degree of directionality (Lay) (Smith, 2008).	87
Figure 2.24	Typical lay types on a machined surface (Groover, 2020).	87
Figure 2.25	Anticipated process roughness and their respective grades (Smith, 2008).	90
Figure 2.26	Burrs produced in planar milling (Chu & Dornfeld, 2005)	93
Figure 2.27	A projection of definitive screening designs (DSDs) for three out of five factors, with a total number of 13 runs.	107
Figure 3.1	Research flow in low-resolution format	114
Figure 3.2	The general dimensions and features of the prepared machining stocks (a) and illustrative image of workpieces prior to adjustments (b).	116

Figure 3.3	Generic representation of ISO/ANSI 490R-08T308M-PL 1010 milling insert	117
Figure 3.4	Three-axis vertical machining centre Mazak Nexus 410A-II where all experimental processes were performed.	118
Figure 3.5	Illustrative geometry of CoroMill® 490 end mill (Sandvik Coromant)	120
Figure 3.6	Research equipment IR Thermographic Camera ThermoPro™ TP8	122
Figure 3.7	Workpiece fixture of the actual machining process (the cutting process was paused for documentation purposes).	126
Figure 3.8	Layout of the experimental setup during the actual machining part of the research.	128
Figure 3.9	Machined part geometry and its illustrated relative position on the milling stock	129
Figure 3.10	General representation of the workpiece and machined part dimensions	129
Figure 3.11	Tool trajectory for open pocket lateral wall (Cutter moved in the given order by following the direction of the arrows, travelling continuously from point 1 to 6).	130
Figure 3.12	Tool trajectory for the thin-walled feature of the pocket (Cutter moved in the given order by following the direction of the arrows, travelling continuously from point 1 to 5).	131
Figure 3.13	Axial depth of cut setup for roughing $ADOC_r$ step (A) and for surface finishing $ADOC_{fs}$ step (B). All units are in mm.	133
Figure 3.14	Schematic illustration for radial depth of cut setups of roughing (A) and surface finishing (B).	133
Figure 3.15	The relative position of retract-plane (A) and feed-plane (B) from the workpiece.	134
Figure 3.16	Responses measurement for the thin-walled feature-related dimensions.	138
Figure 3.17	Selected areas for surface roughness R_a observations of: pocket floor (grey-coloured), pocket wall (polka dots-patterned), and thin wall (wavy-patterned).	139

Figure 4.1	2D Toolpaths interface in Mastercam® software	143
Figure 4.2	Applicable tool path for the end milling of workpiece's open pocket; (a) pocket contour, (b) island contour. The arrow along each tool path indicates tool feed direction.	145
Figure 4.3	Interface of Mastercam® cutting parameters setup for cutter compensation	146
Figure 4.4	Normal probability plot for feeding time <i>FT</i> model in Research Part I.	154
Figure 4.5	Residuals vs. predicted plot (without data transformation) for feeding time <i>FT</i> model in Research Part I	155
Figure 4.6	The DFFITS vs. Run (without data transformation) for feeding time <i>FT</i> model in Research Part I	156
Figure 4.7	Box-cox diagnostic for feeding time <i>FT</i> model in Research Part I	157
Figure 4.8	Normal probability plot for feeding time <i>FT</i> model in Research Part I with Natural Log transformation	161
Figure 4.9	Residuals vs. Predicted plot (with Natural Log transformation) for feeding time <i>FT</i> model in Research Part I	162
Figure 4.10	The DFFITS vs. Run (without Natural Log transformation) for feeding time <i>FT</i> model in Research Part I	163
Figure 4.11	Perturbation plot of feeding time <i>FT</i> in Research Part I	164
Figure 4.12	One-factor effect graph for axial depth of cut during the roughing process (<i>ADOC-r</i>) against feeding time <i>FT</i> .	165
Figure 4.13	One-factor effect graph for number of finishing step (<i>ADOC-fc</i>) against feeding time <i>FT</i>	166
Figure 4.14	One-factor effect graph for number of finishing step in radial cutting (<i>RDOC-fc</i>) against feeding time <i>FT</i>	166
Figure 4.15	One-factor effect graph for feeding-plane incremental distance (<i>FPD</i>) against feeding time <i>FT</i>	167
Figure 4.16	Perturbation plot of all factors for rapid time <i>RT</i> response (Research Part I)	174
Figure 4.17	One-factor effect graph of <i>RDOC-fc</i> for rapid time <i>RT</i> response (Research Part I)	175

Figure 4.18	One-factor effect graph of $ADOC_{fc}$ for rapid time RT response (Research Part I)	176
Figure 4.19	One-factor effect graph of RPD for rapid time RT response (Research Part I)	177
Figure 4.20	One-factor effect graph of $ADOC_r$ for rapid time RT response (Research Part I)	178
Figure 4.21	One-factor effect graph of FPD for rapid time RT response (Research Part I)	179
Figure 4.22	One-factor effect of feed rate $v_f(OP)$ towards cutting temperature $T_c(OP)$	189
Figure 4.23	One-factor effect plot for the quadratic term of depth-of-cut DOC_r^2 during the roughing operation	190
Figure 4.24	One-factor effect plot of cutting speed $v_c(OP)$ towards cutting temperature $T_c(OP)$ in the machining of pocket wall feature	191
Figure 4.25	One-factor effect plot of depth-of-cut DOC_f for finishing operation towards cutting temperature $T_c(OP)$ in the machining of pocket wall feature	191
Figure 4.26	Contour plot of interaction effect between cutting speed $v_c(OP)$ and depth-of-cut DOC_f in the machining of pocket wall feature	192
Figure 4.27	3D Surface graph of cutting speed $v_c(OP)$ and depth-of-cut DOC_f interaction against cutting temperature $T_c(OP)$	193
Figure 4.28	One-factor effects plot of depth-of-cut DOC_r towards the cutting temperature $T_c(TW)$	196
Figure 4.29	One-factor effects plot of cutting speed $v_c(TW)$ towards the cutting temperature $T_c(TW)$	197
Figure 4.30	One-factor effects plot of feed rate $v_f(TW)$ towards the cutting temperature $T_c(TW)$	197
Figure 4.31	Contour plot of cutting temperature $T_c(TW)$ from the interaction of depth of cut DOC_r and cutting speed $v_c(TW)$	198
Figure 4.32	Response surface of cutting temperature $T_c(TW)$ from the interaction of depth of cut DOC_r and cutting speed $v_c(TW)$	199
Figure 4.33	Contour plot of cutting temperature $T_c(TW)$ from the interaction of depth of cut DOC_r and feed rate $v_f(TW)$	200

Figure 4.34	Response surface of cutting temperature $T_c(TW)$ from the interaction of depth of cut DOC_r and feed rate $v_f(TW)$	200
Figure 4.35	The transition of cutting temperature $T_c(OP)$ with depth of cut DOC_r of 0.3 mm. The legend below the graph indicates the number of the run followed by the level of $v_c(OP)$, $v_f(OP)$, and DOC_f , respectively	202
Figure 4.36	The transition of cutting temperature $T_c(TW)$ with cutting speed $v_c(TW)$ of 122.43 m/min. The legend below the graph indicates the number of the run followed by the level of $v_f(TW)$, DOC_r and DOC_f , respectively	204
Figure 4.37	One-factor effect plot of feed rate $v_f(OP)$ towards the deviation W_w of thin wall feature	209
Figure 4.38	One-factor effect plot of depth of cut DOC_r towards the deviation W_w of thin-walled feature	210
Figure 4.39	One-factor effect plot of depth of cut DOC_f towards the deviation W_w of thin-walled feature	211
Figure 4.40	One-factor effect plot of cutting speed $v_c(TW)$ towards the deviation W_w of thin wall feature	212
Figure 4.41	One-factor effect plot of feed rate $v_f(TW)$ towards the deviation W_w of thin wall feature	213
Figure 4.42	One-factor effect plot of feed rate $v_f(OP)$ against the deviation W_{pw}	216
Figure 4.43	Contour plot of deviation W_{pw} response under the influence of cutting speed $v_c(OP)$ and feed rate $v_f(OP)$	217
Figure 4.44	Response surface of deviation W_{pw} response under the influence of cutting speed $v_c(OP)$ and feed rate $v_f(OP)$	217
Figure 4.45	One-factor effect plot of reduced linear model for surface roughness $Ra(FL)$	224
Figure 4.46	Contour plot of surface roughness $Ra(OP)$ from the interaction of $v_c(OP) \times DOC_r$	228
Figure 4.47	Response surface of surface roughness $Ra(OP)$ from the interaction of $v_c(OP) \times DOC_r$	229
Figure 4.48	Contour plot of surface roughness $Ra(OP)$ from the interaction of $v_f(OP) \times DOC_r$	230

Figure 4.49	Response surface of surface roughness $Ra(OP)$ from the interaction of $v_f(OP) \times DOC_r$	231
Figure 4.50	One-factor effect plot of depth of cut DOC_f towards surface roughness $Ra(TW)$	234
Figure 4.51	One-factor effect plot of cutting speed $v_c(TW)$ towards surface roughness $Ra(TW)$	235
Figure 4.52	Contour plot surface roughness $Ra(TW)$ based on the interaction of $DOC_r \times v_f(TW)$	236
Figure 4.53	Response surface of surface roughness $Ra(TW)$ based on the interaction of $DOC_r \times v_f(TW)$	237
Figure 4.54	Lay indications of the three open pocket features: (a) circular lay pattern of pocket floor, (b) parallel lay pattern of lateral pocket wall, and (c) parallel lay pattern of thin wall feature	240
Figure 4.55	Built-up edge (BUE) marks on the lateral pocket wall of (a) Run #8 ($v_c(OP)$ 126.92 m/min; $v_f(OP)$ 152.65 mm/min; DOC_r 0.30 mm, DOC_f 0.05 mm); and (b) Run #5 ($v_c(OP)$ 117.94 m/min; $v_f(OP)$ 610.56 mm/min; DOC_r 0.20 mm, DOC_f 0.05 mm)	242
Figure 4.56	Burr formation on the (a) lateral pocket wall of Run #11 and #8, and on the (b) pocket floor of Run #3 and #4; (c) Enlarged inset picture of the pocket wall burr formation (Run #3, in red)	244
Figure 4.57	Stress patterns and feed marks that can be found in all machining runs, defining the intersection of adjacent features between pocket floor and thin-walled feature	246
Figure 4.58	Flank wear observations of all experimental runs	249
Figure 4.59	Flank wear observations of all experimental runs	252
Figure 4.60	Comparative results of rake wear area	253

LIST OF ABBREVIATIONS

AISI	American Iron and Steel Institute
ANN	Artificial Neural Network
ANOVA	Analysis of Variance
ANSI	American National Standards Institute
BUE	Built-Up Edge
CAD	Computer-Aided Design
CAM	Computer-Aided Manufacturing
CBN	Cubic Boron Nitride
CFRP	Carbon-Fibre Reinforced Plastic
CNC	Computer Numerical Control
DFFITS	Difference in Fits
DIN	<i>Deutsches Institut für Normung</i> eV (German Institute for Standardization)
DOE	Design of Experiment
DSD	Definitive Screening Design
FEM	Finite Element Method
HRC	Rockwell C Hardness
HSS	High Speed Steel
HV	Vickers Pyramid Number
ISO	International Organization for Standardization
MRR	Material Removal Rate
NC	Numerical Control
PCBN	Polycrystalline Cubic Boron Nitride
PCD	Polycrystalline Diamond
PVD	Physical Vapor Deposition
RSM	Response Surface Methodology
VM	Virtual Machining
VMC	Vertical Machining Centre

LIST OF SYMBOLS

$ADOC$	Axial depth of cut (mm)
$ADOC-r$	Axial depth of cut for roughing processes (mm)
$ADOC-fc$	Number of finishing step for axial depth of cut (step)
$ADOC-fs$	Axial depth of cut for surface finish (mm)
D_c	Tool cutting diameter (mm)
FPD	Cutting feed-plane incremental distance (mm)
l_F	Feeding length during one machining process
l_R	Rapid length during one machining process
R_a	Mean surface roughness (μm)
$RDOC$	Radial depth of cut (mm)
$RDOC-fc$	Number of finishing step in radial cutting (mm)
$RDOC-fs$	Radial depth of cut for surface finish (mm)
RPD	Retract-plane incremental distance
t_F	Feeding time (min)
t_R	Rapid (motion) time (second)
T_c	Machining cutting temperature ($^{\circ}\text{C}$)
v_c	Cutting speed (m/min)
v_{cf}	Cutting speed for surface finish (m/min)
v_f	Feed rate (mm/min)
v_{ff}	Feed rate for surface finish (mm/min)
W_p	Dimension deviations for overall pocket width (mm)
W_{pw}	Dimension deviations of thin walled relative position (mm)
W_w	Dimension deviations of thin-walled feature's width (mm)